Published by Avanti Publishers

Journal of Chemical Engineering Research Updates

ISSN (online): 2409-983X

Characterization and Analysis of Gas-Solid Flow Dynamics in Fluidized Bed Systems

Elaine Marinela Gonçalves de Araújo[1], Emerson Barros[1] and A. A. Chivanga Barros[1,2,*]

[1]*Curso de Mestrado em Engenharia de Petróleo, Instituto Superior Politécnico de Tecnologias e Ciências (ISPTEC), Av. Luanda Sul, Rua Lateral Via S10, Talatona - Luanda Sul- República de Angola*

[2]*Centro de Pesquisa e Desenvolvimento (CpD) da Sonangol, Rua Rainha Ginga Nº29/31, Luanda Sul- República de Angola*

ARTICLE INFO

Article Type: Research Article

Academic Editor: Wei He

Keywords:
Fluidization
Fluidized bed
Terminal velocity
Gas-solid interaction

Timeline:
Received: October 30, 2024
Accepted: December 03, 2024
Published: December 19, 2024

Citation: de Araújo EMG, Barros E, Barros AAC. Characterization and analysis of gas-solid flow dynamics in fluidized bed systems. J Chem Eng Res Updates. 2024; 11: 66-79.

DOI: https://doi.org/10.15377/2409-983X.2024.11.4

ABSTRACT

Fluidization is a critical process in various industrial applications, particularly in the oil and gas sector, where it plays a pivotal role in optimizing production, phase separation, and the efficiency of mass and heat transfer, as well as chemical reactions involved in physical and chemical operations. The significance of fluidization stems from its direct impact on key parameters such as pressure drop, flow velocity, particle concentration, and void fraction in multiphase flows. In this context, fluidization enhances the interaction between fluid and solid particles, reducing resistance to heat and mass transfer and promoting material homogenization. This experimental study aims to investigate the flow behavior of a particulate system within a fluidized bed, specifically focusing on the fraction of the continuous (gas) phase relative to a defined volume of solid particles. The results obtained, when compared to existing literature primarily concerned with the effects of particle size and flow rate on fluidization, demonstrate consistency in both qualitative and quantitative analyses. These findings suggest that the increase in the volume of the continuous phase in such flows is strongly influenced by the Reynolds number and the particle size within the system. Thus, this study makes significant contributions to the optimization of fluidization processes, particularly in industrial sectors like oil and gas. By providing detailed experimental insights into the factors that influence fluidized bed performance, the findings offer practical implications for improving the efficiency of heat and mass transfer, phase separation, and reaction rates in industrial applications where the behavior of the continuous phase is crucial.

*Corresponding Author
Email: chivanga.barros@isptec.co.ao
Tel: +(244) 928 727 901

1. Introduction

Over the years, fluidized bed reactors have become increasingly pivotal in both scientific and advanced industrial applications due to their enhanced operational flexibility and process efficiency. The concept of the fluidized bed reactor was first introduced by A. M. McAfee in 1915, who applied it to fluidized catalytic cracking (FCC) to optimize gasoline production in oil refineries [1-4].

The impact of fluidized bed reactors has led to significant scientific and technological advancements that have, in turn, spurred industrial development globally. Fluidization, in its broad application, has been employed in various processes, including the drying and storage of solids, the removal of sulfur and heavy metals during oil processing, thermal and catalytic cracking, and the intensification of industrial processes. Consequently, the integration of fluidization into industrial processes, particularly in the development of new technologies, necessitates improvements in process stages to enhance efficiency and minimize environmental impacts [5-9].

In the oil and gas industry, fluidized bed reactors are indispensable for thermal and catalytic cracking operations, particle coating, and the development of catalysts for chemical reactions. The distinctive characteristics of these reactors have facilitated the development of models aimed at optimizing and controlling fluid-dynamic behavior in single-phase, two-phase, and multiphase flow systems. A critical factor in this control is bubble formation, as the presence of bubbles in fluidization processes can significantly affect the operational behavior of valves along production pipelines. The formation of larger diameter bubbles, which can travel at higher velocities compared to smaller ones, necessitates stringent control measures [10-15].

Fluidization processes are fundamentally governed by the physical state of the involved phases and the interplay of forces, which adhere to the principles of phase equilibrium. These processes can be categorized into gas-liquid, gas-solid, liquid-solid, and liquid-liquid flow systems [16-20]. This study focuses on gas-solid flow within a fluidized bed, where fluidization involves the movement of gas as the continuous phase and solid particles as the dispersed phase, which behaves fluid-like upon interaction with the continuous phase [21-28].

A comprehensive understanding of fluidization principles is essential for ensuring the efficiency and safety of processes in the oil and gas industry, making it a critical area of study within engineering [29-31]. When applied to oil and gas processes, fluidization significantly enhances mass and heat transfer rates [32-35]. This results in practical benefits, such as the substantial reduction of agglomeration and fouling issues, thereby greatly improving process efficiency [36, 37]. Another significant outcome of fluidization is the maximization of oil recovery efficiency in mature reservoirs [27, 38-42]. Furthermore, fluidization allows for adaptation to the specific characteristics of various oil fields and operating conditions, ensuring process versatility and reliability. However, implementing fluidization in oil and gas industry processes requires precise control of operating conditions to mitigate challenges such as solids entrainment and the detrimental effects of sulfur and metals present in the oil [19, 28, 35, 43-47].

To advance oil and gas industry processes, it is imperative to focus on the development of fluidization technologies, process optimization, cost reduction, and the minimization of environmental impacts [14, 48, 49]. These objectives have driven recent research into modern fluidization techniques and equipment [15, 50]. For effective application, two-phase fluid flow models must accurately represent the physical phenomena governing phase interactions to uphold the continuity principles in two-phase flows [51, 52]. Accordingly, Equation (1) defines the mass density of phase N within an infinitesimal control volume (δVo), which is used to describe the mass distribution of each phase within a small control volume [53-55].

$$\rho_N = \lim_{\delta V \to \delta V_o} \frac{\delta m_N}{\delta V} \tag{1}$$

Where δV_o is the volume that guarantees a certain uniformity, measured over a time interval δt_o. The volume fraction (α_N) of a given phase N, is defined according to Equation (2) [56].

$$\alpha_N = \lim_{\delta V \to \delta Vo} \frac{\delta V_N}{\delta V} \tag{2}$$

The concept described in Equation (2) is crucial in the study of multiphase and two-phase flows, as it is used to characterize the spatial distribution of the phases within the flow system. The volume fraction, denoted as α_N, represents the proportion of the total volume δV that is occupied by phase N. This dimensionless parameter ranges from 0 to 1, providing a precise measure of the phase distribution within a control volume. Equation (2) considers an infinitesimal control volume δVo, which allows for an accurate representation of the volume fraction, making it essential for detailed flow modeling. In this context, the volume fraction of the dispersed phase, α_D, is often referred to as the void fraction. In the oil and gas industry, a key application of this concept is in the analysis of the volume fraction of the liquid phase, commonly known as liquid holdup, which is a critical parameter in two-phase gas-liquid flow systems, as described by Equation (3) [57].

$$\alpha_G + \alpha_L = 1 \tag{3}$$

In this context, the void fraction (α_G) represents the continuous phase, while the dispersed fraction (α_L), also known as liquid holdup, represents the dispersed phase. These volume fractions are integral to the equations governing the conservation of mass, momentum, and energy for each phase. In two-phase flow, the terms are expressed using α_N to account for the specific contributions of each phase.

The volume fraction is a critical parameter that directly influences the interactions between the phases, as well as the interfacial forces and flow dynamics [58, 59]. In two-phase flows, the volume fractions of the dispersed and continuous phases are determined by the interface between the phases and the associated dynamic processes [60, 61]. Accurately determining the volume fraction is essential for modeling and simulating these interactions. In numerical methods, particularly Computational Fluid Dynamics (CFD), the volume fraction is a key parameter used to simulate multiphase flows [40, 62]. It enables a detailed representation of the interfaces and the spatial distribution of the phases, providing valuable insights into the complex behaviors of multiphase systems [63, 64]. The volumetric flow rate (Q) in Equation (4) and the volumetric flow or surface velocity (j) are related by the area of the straight cross-section of the pipe (A) [65].

$$j = \frac{Q}{A} \tag{4}$$

Where A is defined according to Equation (5).

$$A = \frac{\pi d^2}{4} \tag{5}$$

Where d is the diameter of the circular area. For this case, the relative velocity of the flow involves the sum of the *in-situ* velocities (Equation 6) [66].

$$u_{AB} = u_A + u_B \tag{6}$$

For high concentrations, the particle flow field is modified by the particle-fluid interaction. In addition, the volumetric flow of the dispersed phase cannot be negligible, as it can cause a non-negligible flow of the continuous phase. The average particle velocity causes a positive flow of the dispersed phase $j_L = -j_G$ and so the average velocity of the continuous phase is given by Equation (7) [67].

$$u_L = \frac{j_L}{\alpha_L} \tag{7}$$

Therefore, the relative velocity between the dispersed and continuous phases is described according to Equation (8) [67].

$$u_{GL} = u_G - u_L = \frac{j_G}{\alpha_G} - \frac{-(j_G)}{\alpha_L} = \frac{j_G}{\alpha_G \alpha_L} = \frac{\alpha_G u_G}{\alpha_G(1-\alpha_G)} = \frac{u_G}{1-\alpha_G} \tag{8}$$

In this way, terminal velocity encompasses the moment when particles fall into a fluid under the action of a constant force, such as the force of gravity, and gain acceleration for a very short period of time, after which they move at a constant speed (Equation 9).

$$v_t = -(u_G - u_L) \tag{9}$$

The measure of the type of flow is based on turbulence phenomena, measured through the Reynolds number of the dispersed phase, associated with the relative velocity between the phases (Equation 10) [57].

$$N_R = \frac{\rho_G d_p |u_G - u_L|}{\mu_G} \tag{10}$$

Where N_R is the Reynolds number, ρ_G is the density of the continuous phase, d_p is the particle diameter, u_G is the superficial velocity of the continuous phase, u_L is the superficial velocity of the dispersed phase, and μ_G is the dynamic viscosity of the continuous phase. Richardson and Zaki [21] proposed an equation that relates the dispersed phase, incorporating the effects of the wall, as shown in Equation (11).

$$\psi(\alpha_L) = (1 - \alpha_L)^{-n} \tag{11}$$

Where $\psi(\alpha_L)$ is a function of the volume fraction of the dispersed phase, α_L, and *n* is a constant that governs the system's behavior, typically based on empirical or experimental data. Wall effects can be evaluated using Equation (12), described as a ratio between the diameters of the particle and the duct, according to the correlation proposed by Reynolds, for an established range of Reynolds numbers [56].

$$n = 4.45 N_R^{-0.1} \rightarrow 200 < N_R < 500 \tag{12}$$

During fluidization, the particles separate and remain suspended when a fluidized bed is formed. This condition involves fluidization regimes that encompass different states of these phenomena, as described in Fig. (**1**).

For this reason, each fluidization regime exhibits distinct phenomenological characteristics that significantly influence the fluidization process and the operation of industrial equipment [68, 69]. The interaction between particles and the fluid within the fluidized bed is primarily driven by changes in fluid velocity. At low fluid velocities, the bed is characterized by a dense suspension of particles with minimal drag forces acting on them [70]. However, as the fluid velocity increases, the dense surface of the bed begins to break down, leading to significant particle drag and a more turbulent system (Fig. **2**) [22, 71].

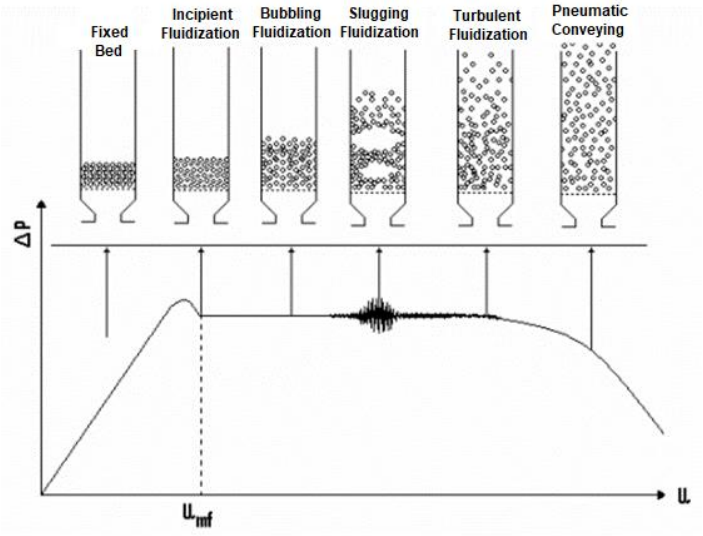

Figure 1: Fluidization regimes as a function of the gas superficial velocity [12].

Ommen *et al*. [42] utilized pressure drop data and high-speed camera imaging to map flow regimes in fluidized beds fabricated at various scales. Their findings indicated that the rough surfaces, induced by additives during the manufacturing process, do not significantly affect fluidization characteristics or wall effects in small-scale beds [58]. The analysis of fluidized bed flow, considered as a particle flow field associated with terminal velocity, should take into account the pressure drops as a function of increasing superficial gas velocity. This pressure drop serves as a transition point between bubbling and the bubbling-to-slugging regime (Fig. **2**). At this transition point, bubble expansion ceases, but any further increase in superficial velocity leads to a decrease in the bed's pressure drop. Under these conditions, the total pressure drop remains approximately constant because the contribution of the fixed bed's pressure drop diminishes compared to that of the bubbling bed [71-74].

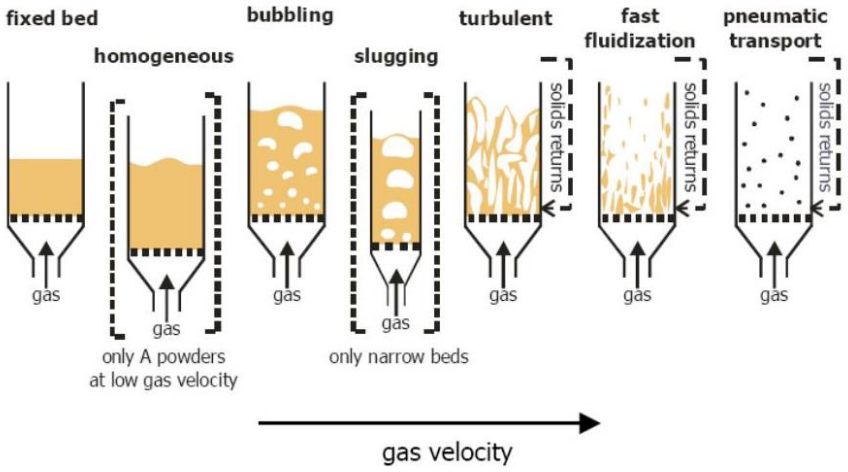

Figure 2: Flow regimes produced in a fluidized bed [42].

Terminal velocity is a key parameter in fluidization, with several empirical and semi-empirical correlations incorporating both the minimum fluidization velocity and the head loss in the bed. The distribution pattern of particle concentration is primarily controlled by the interplay between terminal velocity and shear velocity. Zhou and Yang [75] and Nawaz *et al*. [45] observed that for a given shear velocity, the mobility of the particulate system is characterized by greater sedimentation of larger particles. Conversely, for a fixed terminal velocity and particle size, a reduction in shear velocity decreases particle mobility, leading to a rapid decrease in sediment concentration with increasing vertical distance. In this context, Michael *et al*. [76] conducted studies to determine the minimum and terminal velocities at varying temperatures for a porous and inert material (ceramic) produced by the calcination of clay in an oxidizing environment. The study found that the minimum fluidization velocity generally decreases with increasing temperature, except for particles with diameters greater than 2.25 mm. The phenomena evaluated exhibited a linear relationship between the flow system's temperature and the size of the particles under evaluation.

To enhance the consistency of their analysis, Michael *et al*. [76] proposed mathematical correlations to estimate the particle size required for achieving desired velocities, with potential applications in engineering projects involving the fluidization of ceramic and similar materials. In their studies, terminal velocities were measured in triplicate and compared with entrainment velocities, revealing that entrainment velocities reduce flow velocity by 2% to 6%. This study examined flow velocities ranging from 0.5 m/s to 2.5 m/s at room temperature. The findings suggest that particle size significantly influences the fluidization regime, as smaller particles require higher velocities to achieve the appropriate fluidization regime.

Scatena and Cremasco [43] employed numerical simulation based on computational fluid dynamics (CFD) principles to evaluate the dynamics of a mathematical model of a fluidized bed using chaos theory in a time series of pressure drops under minimum fluidization conditions for the three types of particles classified by Geldart [3]. The principles outlined in their work enhance the understanding of fluidized bed behavior under different experimental conditions, contributing to the advancement of knowledge in this area. In this context, gas-solid fluidization experiments were conducted to identify the involved phenomena, particularly those characterized by

intense bubbling, increased pressure loss, and the increased presence of the continuous phase within the discontinuous phase. These parameters allowed for the determination of the fractions of the continuous and dispersed phases, present in the system [26, 77-80].

2. Materials and Methods

The experimental tests were conducted using both qualitative and quantitative approaches, utilizing the "Fluidized Bed Formation (CE 220)" apparatus from Gunt, which served as the cornerstone of our research into gas-solid fluidization. This apparatus was instrumental in investigating fluidization phenomena, with the system incorporating particles with a diameter of 0.1 µm. The apparatus facilitated the visualization of the fluidized bed as the continuous and ascending phase (air) passed through the initially static dispersed phase within a vertical flow duct supported by a porous symmetrical metal plate.

Before commencing the experimental procedures, the height of the static solid particle mass within the duct was precisely measured using a ruler installed externally along the duct of the experimental apparatus. Following this, the airflow valve was opened, and meticulous readings were taken of the flow rate, system pressure loss, and the maximum height reached by the particles in the duct as they formed a fluidized bed. The measurement of the maximum height was only recorded after ensuring that the airflow from the compressor had stabilized.

Measuring the maximum height reached by the particles in the fluidized bed is crucial for calculating the fractions of the continuous and discontinuous phases within the system. This accurate measurement allows for a precise determination of the system's phase distribution, which is essential for understanding and modeling the fluidization process.

After completing the initial stage, the continuous phase (air) flow rate was systematically increased. Measurements were taken of the pressure drop, air flow rate, and the maximum height of the entrained particles, following the procedure previously described. This process was meticulously repeated until the maximum air flow rate was reached (Fig. **3**), utilizing the experimental apparatus designed for these studies (Fig. **4**).

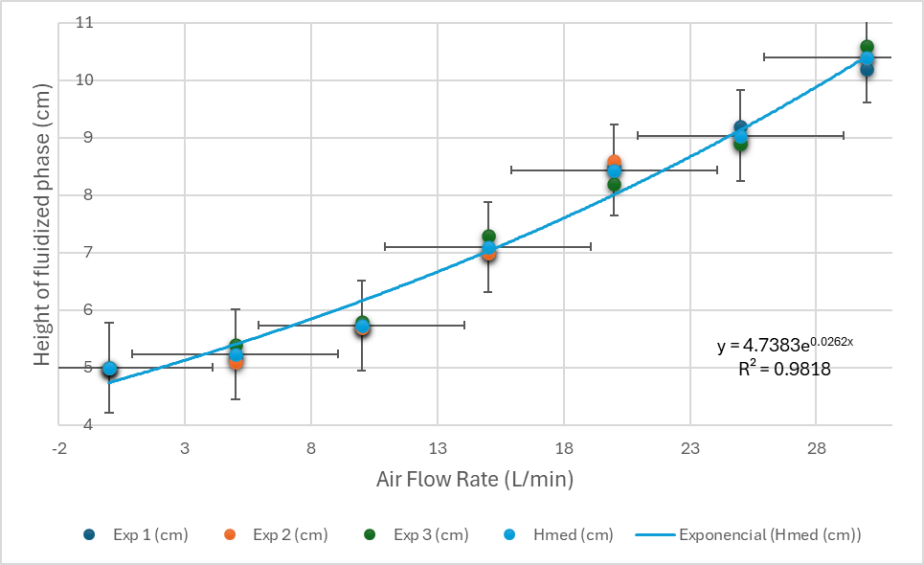

Figure 3: Dates measures, average, and error from the three experiments.

The data obtained from these experimental tests enabled a thorough qualitative and quantitative analysis of the measured parameters, which, in turn, supported the phenomenological studies related to two-phase flow in a fluidized bed. For continuous phase flow, the apparatus was equipped with a compressor capable of delivering a maximum flow rate of 38 L/min. The system also included solid silicon particles (standard from Gunt), with a diameter of 0.1 µm, contained within a glass tube measuring 380 mm in length and 44 mm in internal diameter (Fig. **4**).

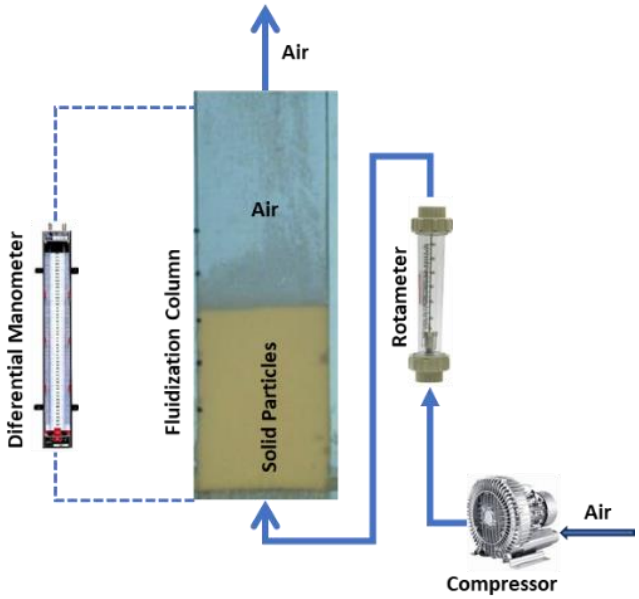

Figure 4: Physical characteristics of the experimental apparatus used in this study.

2.1. Procedures

The calculation procedures employed in these studies involved several key steps. Initially, experimental data were acquired, followed by the calculation of phenomenological properties relevant to the study. Subsequently, profile graphs were prepared, incorporating the evaluated variables to visually represent the relationships and trends observed. The final step involved interpreting the data, which was then rigorously compared with existing data from the literature to ensure accuracy and relevance (Fig. **5**).

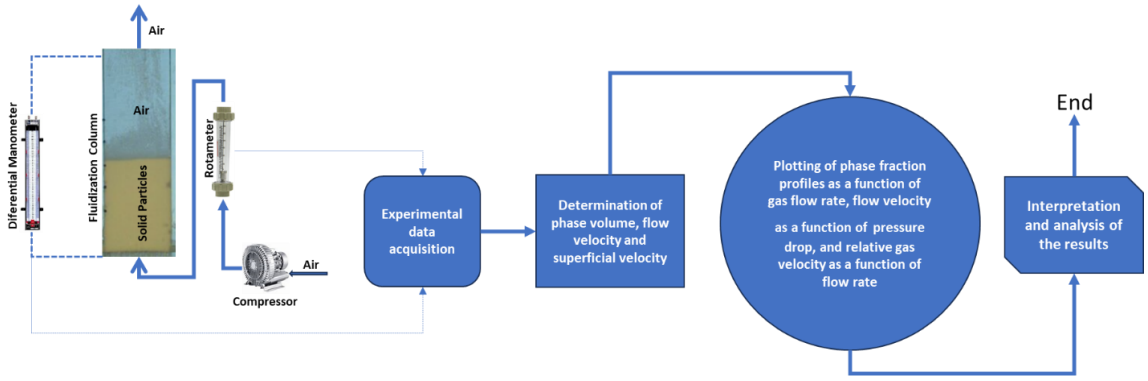

Figure 5: Methodological sequence used to determine the parameters of two-phase flow in a fluidized bed.

The methodological sequence outlined in Fig. (**5**) ensures a systematic and rigorous approach to determining the parameters of two-phase flow in a fluidized bed, offering valuable insights into the fluidization process. Therefore, the calculations performed in this analysis were thoroughly supported by the equations presented in this scientific article, which encompass the properties of the continuous and dispersed phases that were experimentally evaluated in this study. These equations provided a robust framework for analyzing the behavior of the system and ensured that the results were grounded in established scientific principles.

3. Results and Discussion

The graphical analysis of the results in this study involves understanding the profiles of the phase fractions as a function of the airflow rate in the fluidized bed. Initially, the system is characterized by the absence of airflow,

where the dispersed phase fraction (α_D) is equal to 1. In this state, the solid particles remain static, fully occupying the bed. As the experiment progresses, the airflow rate is gradually increased, and the volume level of the fluidized phase inside the duct is monitored. This observation allows for the determination of the phase fractions within the system. As depicted in Fig. (**6**), it is evident that at lower airflow rates, the dispersed phase fraction predominates, indicating a dense, unfluidized bed. However, as the airflow rate increases, the strength of the dispersed phase diminishes, and the continuous phase becomes more dominant. This shift illustrates the transition from a static bed to a fully fluidized state, where the interaction between the phases becomes more dynamic, significantly altering the flow characteristics of the system.

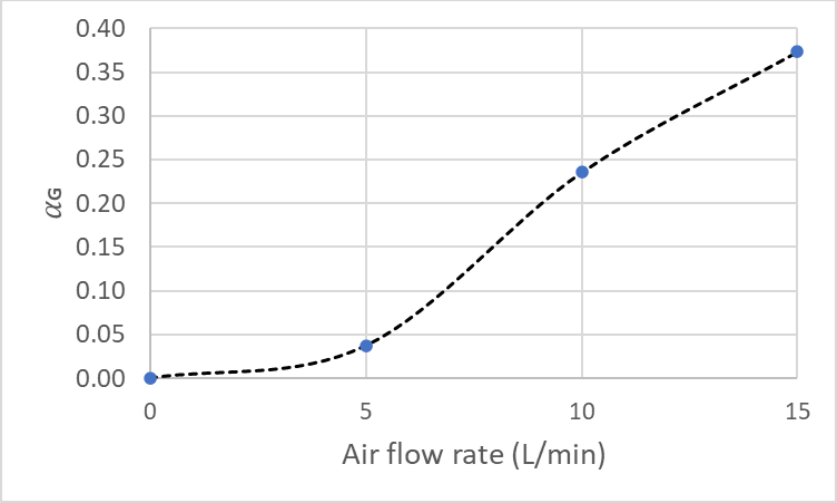

Figure 6: Evolution of continuous phase fractions with increasing air volumetric flow rate.

Therefore, the increase in the volume fractions of the continuous phase leads to a corresponding reduction in the dispersed phase fractions within the fluidized bed, as illustrated in Fig. (**7**). This inverse relationship is directly influenced by particle size, a factor that has been experimentally observed by Michael *et al*. [76]. Their studies highlighted that particle size significantly affects the fluidization regime, with different particle sizes exhibiting distinct behaviors during fluidization. Larger particles tend to require higher airflow rates to achieve fluidization, while smaller particles fluidize more easily but may result in different phase interaction dynamics. This phenomenon underscores the importance of considering particle size in the design and optimization of fluidized bed processes.

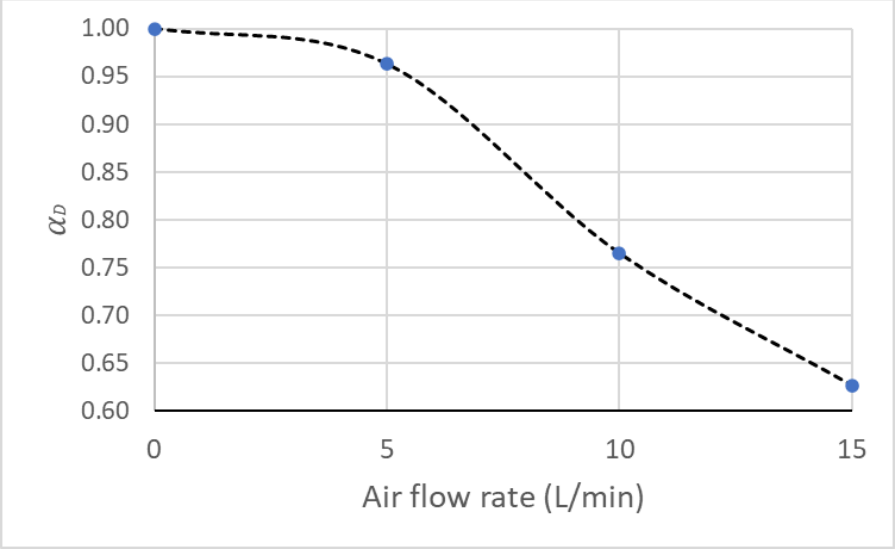

Figure 7: Evolution of the fractions of the dispersed phase, with the increase of the volumetric flow rate of the air.

The analysis of the behavior described in Fig. (**6**) and (**7**) reveals that as velocities decrease, the dispersed phase fractions dominate; however, these fractions diminish as the flow rates increase. Under operating conditions with maximum airflow, fluidization becomes more intense, resulting in the fluid phase prevailing within the system, which is indicative of chaotic flow behavior.

According to Contado [78] and Soares *et al*. [79-80], intrinsic parameters such as size, shape, density, and surface characteristics critically influence a particle's response in a flow field. While average particle dimensions can qualitatively represent size, a more precise and meaningful definition is necessary for calculations. The size of a spherical particle is determined by its diameter, and similarly, the size of regular isotropic particles (such as cylinders, cubes, and spheroids) can be defined by two dimensions. However, in practice, we often encounter irregular three-dimensional particles whose "size" must be uniquely determined. The most logical approach is to define an equivalent diameter, corresponding to a sphere that behaves similarly to the irregular particle when subjected to a given physical process.

The fluidization characteristic curve, which relates the pressure drop to the fluid's surface velocity, shows that an increase in fluid velocity results in a higher pressure drop. However, this parameter stabilizes when the flow rate exceeds 6 L/min, as indicated by the data in Fig. (**8**). Significant pressure drops occur when the particles, characterized as the dispersed phase, agglutinate with reduced porosity. In such cases, higher flow rates of the continuous phase are required to achieve particle dispersion, as observed experimentally. Once the flow rate of the continuous phase increases beyond a certain point, further increases no longer affect the pressure drop. At this stage, the forces acting on the solid particles, including gravitational, buoyancy, and drag forces, become predominant. Additionally, particle-particle interaction forces play a significant role, and these forces often need to be considered in the numerical analysis of such phenomena.

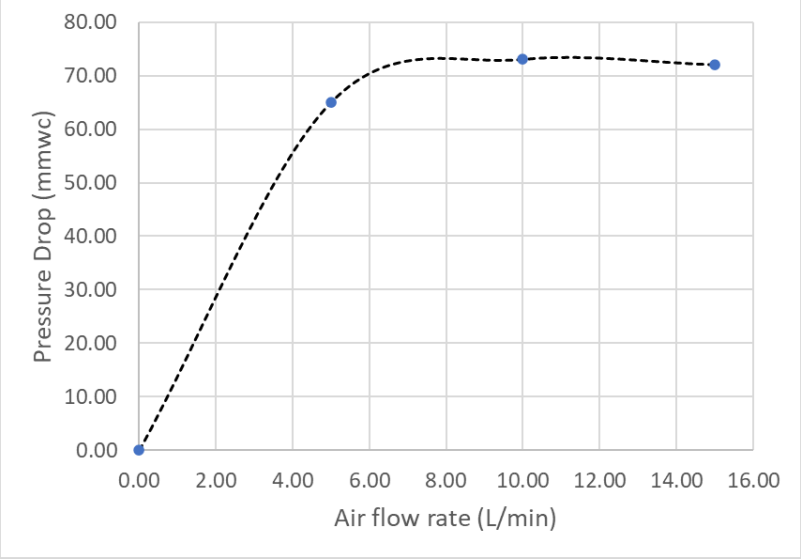

Figure 8: Fluidization characteristic curve from this study.

Jena *et al*. [29] conducted a study primarily focused on evaluating the influence of the composition of the mixture being fluidized on the pressure drop within the bed. The mixtures examined contained particles of varying sizes, and the final results were consistent with those observed in this study, showing an increase in the fraction of the continuous phase as the flow rates of the continuous phase increased.

Additionally, the analysis of the relationship between air flow rates and relative velocity, characterized by a product that includes the fluid's viscosity, particle diameter, and the length of the fluidized bed column, demonstrates that increasing the air flow rate leads to a marked increase in relative velocities across the entire range of flow rates evaluated in this study (Fig. **9**). This relationship highlights the direct impact of gas flow rate on the dynamics of the fluidized bed, reinforcing the importance of controlling flow parameters to optimize the fluidization process and ensure effective operation of the system.

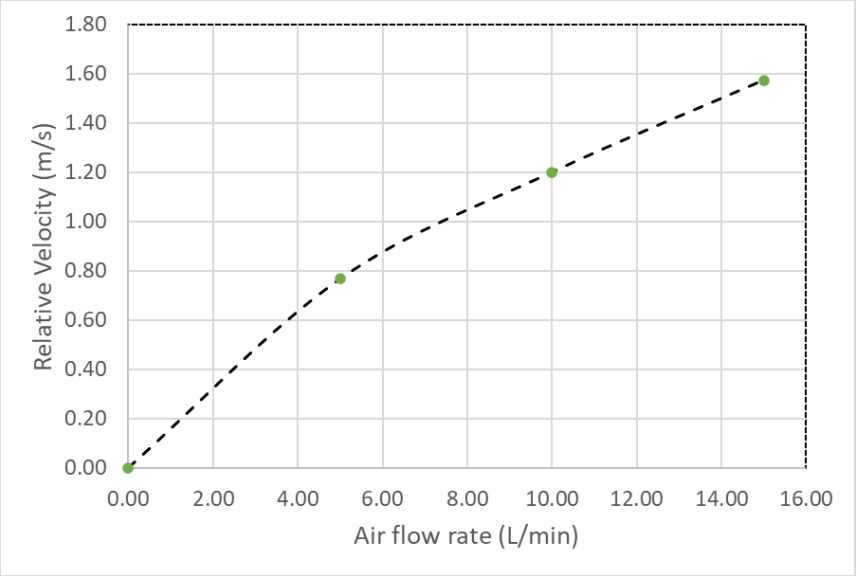

Figure 9: Relation between air flow rate and relative velocity.

Therefore, as shown in Fig. (**6**) and (**7**), the lighter particles tend to float on the surface during fluidization, with a corresponding increase in relative velocity as the flow rate of the continuous phase increases. As velocity rises, the forces acting on the particles become more pronounced, leading to an increase in the pressure drop within the system. At the initial flow rates, this pressure drop is significant, but it stabilizes for flow rates exceeding 8 L/min. Under these conditions, the fluidized bed expands due to increased porosity, while the pressure drop remains constant.

A study conducted by Anantharaman *et al*. [36] determined the minimum fluidization velocity and observed that, with increasing superficial gas velocities, the fluidization curve initially decreases and then stabilizes. This behavior reflects the relationship between the pressure drop in the bed, the mass of the dispersed phase, and the cross-sectional area of the bubbling column involved in the experimental studies.

Thus, fluidization processes involve high pressures and require the determination of key parameters, such as the minimum fluidization velocity, terminal velocity (drag), and the system's bubbling behavior. Table **1** presents the calculated data that underpin the behavior of the fluidization curve observed in this study, offering a quantitative basis for understanding the fluidization dynamics in the system.

Table 1: Parameters involved in calculating terminal velocity.

Q(L/min)	α_G	α_L	H(cm)	Ut (m/s)
0.00	0.00	1.00	5.20	0.00
5.00	0.04	0.96	5.40	0.16
10.00	0.24	0.76	6.80	0.15
15.00	0.37	0.63	8.30	0.14

Calvi [39] observed that after the initial fluidization of the bed, a decline in pressure drop occurs for velocities exceeding the minimum fluidization velocity (U_{mf}). In his study, which involved particles with diameters ranging from 1.3 mm to 4.5 mm, Calvi [39] determined that the minimum fluidization velocities were between 0.5 m/s and 1.65 m/s at atmospheric pressure. For systems pressurized with nitrogen at 0.7 MPa, the minimum fluidization velocities were found to be lower, ranging from 0.28 m/s to 0.75 m/s. This observation highlights the influence of both particle size and system pressure on the fluidization behavior and the corresponding pressure drop in fluidized beds.

Similarly to the data presented by Calvi, the results from this study show a strong influence of the air flow rate on the pressure drop in the fluidized system, as shown in Fig. (**8**), where a significant increase in pressure drop is observed for flow rates below 6 L/min. After this phase, characterized by significant particle agglomeration, an increase in the continuous phase flow rate leads to an improvement in the dispersion degree, where the effects of particle interaction are reduced, resulting in the subsequent stabilization of pressure in the system. Therefore, Fig. (**6**) and (**7**) better illustrate this behavior, characterized by a pronounced increase in the continuous phase in the fluidized bed, a factor that ensures pressure stabilization in the system.

4. Conclusions

Based on the results discussed in this work, the following conclusions can be drawn:

The experimental tests conducted successfully determined the terminal velocities for different flow rates of the continuous phase and established their relationship with the pressure drop within the system.

The fluidization curve obtained from this study is consistent with those reported in the literature, demonstrating the correlation between the flow rate and velocity of the continuous phase and the pressure drop in the system.

The fractions of the continuous phase progressively increase within the fluidized bed system as the flow rates of this phase rise, while an opposite trend is observed in the behavior of the dispersed phase.

The minimum fluidization velocity and the terminal velocity are key phenomenological characteristics of the fluidized bed in multiphase flow systems, and their calculations are essential for the design and development of fluidized bed projects.

The classification of fluidization provides a framework for defining the type of fluidization and analyzing the behavior of fluids in multiphase flow systems, contributing to the understanding and optimization of such processes.

Nomenclature

u_G = velocity of the continuous phase (m/s)

u_L = velocity of the disperse phase (m/s)

j_L = flow rate of the dispersed phase (m^3/s)

j_G = flow rate of the continue phase (m^3/s)

α_L = volume fraction of disperse phase

α_G = volume fraction of continue phase

Q = volumetric flow rate (m^3/min)

A = cross-sectional area (m^2)

d = Tube diameter (m)

N_R = Reynolds number

d_p = particle diameter (m)

ρ_L = density of the disperse phase (kg/m^3)

ρ_G = density of the continuous phase (kg/m^3)

v_t = Terminal velocity (m/s)

μ_G = is the dynamic viscosity of the continuous phase (Pa·s or kg/(m·s))

ΔP = Pressure loss (mmcf);

$\psi(\alpha_L)$ = function of the volume fraction of the dispersed phase

δV = infinitesimal control volume (m^3)

δm_N = infinitesimal control mass (kg)

n = constant that governs the system's behavior

T = temperature (K)

H = Height of the fluidized bed column (m)

Conflict of Interest

The authors declare that there are no competing interests related to the research, authorship, or publication of this manuscript. No financial, personal, or professional relationships, whether direct or indirect, exist that could inappropriately influence the work presented in this study.

Ethical Consideration

The authors further confirm that they have adhered to ethical guidelines in conducting and presenting the research, ensuring that the results and conclusions drawn are unbiased and free from any conflict of interest.

Funding

For the development of this work, no funding was made available, but the joint efforts of all involved made the successful completion of this scientific paper possible.

Acknowledgments

The authors of this work sincerely express their gratitude to the Master's Course in Petroleum Engineering and the Post-Graduation Coordination of ISPTEC for their invaluable collaboration and support.

References

[1] King D. Engineering of Fluidized Catalytic Crackers. Chevron Research and Technology Company; 1993.

[2] McAfee AM. The fluidized bed reactor: a new approach to catalytic cracking. Ind Eng Chem. 1915; 7: 140-7.

[3] Geldart D. Types of fluidizations. powder technol. 2014; 7: 285-92. https://doi.org/10.1016/0032-5910(73)80037-3

[4] Kunii D, Levenspiel O. Fluidization Engineering. 2nd ed. Butterworth-Heinemann; 2013.

[5] Santos JS, Walesiuk N, D'Amelio MTS. Estudo de Leito Fluidizado. Rev Cient Multidiscip Núcleo Conhecimento. 2019: 106-34. https://doi.org/10.32749/nucleodoconhecimento.com.br/educacao/sala-de-aula

[6] Glicksman LR. Scaling relationships for fluidized beds. Powder Technol. 2015; 356: 128-36. https://doi.org/10.1016/0009-2509(84)80070-6

[7] Lu J, Adams TA. Emerging trends in fluidization research. Chem Eng Res Des. 2017; 123: 119-34.

[8] Basu P. Biomass gasification, pyrolysis, and torrefaction: practical design and theory. 2nd ed. Academic Press; 2013. https://doi.org/10.1016/B978-0-12-396488-5.00007-1

[9] Fan LS. Chemical Looping Systems for Fossil Energy Conversions. Wiley-AIChE; 2014.

[10] Cocco R, Karri S, Knowlton T. Introduction to Fluidization. Chem Eng Prog. 2014; 110(11): 21-9.

[11] Zapater D, Kulkarni SR, Cui M, Gascon J, Castaño P, Herguido J, *et al*. Multifunctional fluidized bed reactors for process intensification. Prog Energy Combust Sci. 2024; 105: 101176. https://doi.org/10.1016/j.pecs.2024.101176

[12] Denbigh KG. Velocity and yield in continuous reaction systems. Trans Faraday Soc. 1944; 40: 352. https://doi.org/10.1039/tf9444000352

[13] Grace J, Bi X, Ellis N. Essentials of fluidization technology. John Wiley & Sons; 2020. https://doi.org/10.1002/9783527699483

[14] Van Ommen JR, Nijenhuis J, Coppens M-O. Four approaches to structure gas-solid fluidized beds. 12th International Conference on Fluidization - New Horizons in Fluidization Engineering; 2007.

[15] Kapteijn F, Moulijn JA, Krishna R. The generalized Maxwell-Stefan model for diffusion in zeolites: sorbate molecules with different saturation loadings. Chem Eng Sci. 2000; 55: 2923-30. https://doi.org/10.1016/S0009-2509(99)00564-3

[16] Smith G, Taylor J. Gas-solid fluidization: basic principles and applications. Chem Eng Sci. 2020; 45(2): 123-35.

[17] Johnson H, Williams M. Multiphase flow in fluidized beds: models and applications. Int J Multiphase Flow. 2019; 34(5): 567-89.

[18] Anderson L, Pate P. Fluidization in the oil and gas industry: benefits and challenges. Energy Fuels. 2018; 33(8): 1678-90.

[19] Kumar A, Sharma S. Impact of fluidization on heat transfer in oil refining processes. J Pet Eng. 2019; 45(3): 392-407.

[20] Noriler D, Meier HF, Barros AAC, Maciel MRW. Thermal fluid dynamics analysis of gas–liquid flow on a distillation sieve tray. Chem Eng J. 2008; 136(2-3): 133-43. https://doi.org/10.1016/j.cej.2007.03.023

[21] Richardson JF, Zaki WN. Sedimentation and fluidisation. Part I. Trans Inst Chem Eng. 1979; 32: 35-53.

[22] Cheng J, Fan X, Fan S, Jingyuan Y, Yao H, Zhengliang W, *et al*. Evolution and fluidization behaviors of wet agglomerates based on formation-fragmentation competition mechanism. Chem Eng Sci. 2022; 247: 11. https://doi.org/10.1016/j.ces.2021.116933

[23] Cocco R, Issangya A, Reddy SB, Freema TH, Jaeger M, Knowlton TM. Small-scale particle interactions are having significant effects on global fluidized bed behavior. KONA Powder Part J. 2017; 34: 155-67. https://doi.org/10.14356/kona.2017021

[24] Brown C, Green P. Fluidized Bed Reactors in Petroleum Processing. Fuel Process Technol. 2018; 126: 23-34.

[25] Taylor D, Collins M. Gas-solid flow and fluidization behavior in bed systems. Chem Eng Res Des. 2017; 45(9): 980-91.

[26] Zhang E, Wang F. Improved fluidization models for enhanced heat transfer in oil production. J Chem Eng Technol. 2021; 42(11): 2097-111.

[27] Miller S, Reynolds B. Optimization of oil recovery via fluidized bed technology. Soc Pet Eng J. 2022; 63(2): 945-57.

[28] Singh P, Mehta K. Control of solids entrapment and metal contamination in fluidized systems. Environ Eng Sci. 2019; 48(3): 532-44.

[29] Jena HM, Roy GK, Biswal KC. Studies on pressure drop and minimum fluidization velocity of gas–solid fluidization of homogeneous well-mixed ternary mixtures in un-promoted and promoted square bed. Chem Eng J. 2008; 145: 16-24. https://doi.org/10.1016/j.cej.2008.02.013

[30] Noriler D, Meier HF, Barros AAC, Maciel MRW. Thermal fluid dynamics analysis of gas–liquid flow on a distillation sieve tray. Chem Eng J. 2008; 136(2-3): 133-43. https://doi.org/10.1016/j.cej.2007.03.023

[31] Harrison M, Douglas P. Engineering fluidized bed systems for oil refining. Energy Fuels. 2021; 35(7): 2043-55.

[32] Rhodes MJ. Introduction to particle technology. John Wiley & Sons; 2008. https://doi.org/10.1002/9780470727102

[33] Soares C, Noriler D, Wolf Maciel MR, Barros AAC, Meier HF. Verification and validation in CFD for a free-surface gas-liquid flow in channels. Braz J Chem Eng. 2008; 30: 323-5. https://doi.org/10.1590/S0104-66322013000200010

[34] Harris F. A review on fluidization and its application in oil recovery. J Pet Technol. 2020; 59(8): 634-42.

[35] Gupta H, Desai P. Managing sulfur and metal contamination in fluidized systems for oil refining. Chem Eng Sci. 2022; 99: 210-24.

[36] Anantharaman A, Cocco R, Chew A, Wei J. Evaluation of correlations for minimum fluidization velocity (Umf) in gas-solid fluidization. Powder Technol. 2018; 323: 454-85. https://doi.org/10.1016/j.powtec.2017.10.016

[37] Lee D, Thompson E. Addressing fouling and agglomeration in fluidized beds for refining processes. Ind Eng Chem Res. 2021; 59(9): 1849-62.

[38] Zhow Y, Wang T, Zhu J. Development of gas-solid fluidization particulate and aggregative. Powder Technol. 2023; 421: 118420. https://doi.org/10.1016/j.powtec.2023.118420

[39] Calvi FA. Estudo da fluidodinâmica de uma mistura de sólidos em um leito fluidizado gás-sólido. Trabalho de conclusão de curso. Universidade Estadual Paulista (Unesp); 2013.

[40] Miller HL, Brown JP. Application of computational fluid dynamics in multiphase flow simulations. J Appl Mech. 2022; 72(10): 1243-55.

[41] Patel G, Singh R. Enhancement of oil recovery using fluidized bed technologies. Energy Fuels. 2020; 39(5): 1901-15.

[42] Ommen JV-R, Sasic S, Schaaf JV-D, Gheorghiu S, Johnsson F, Coppens MO. Time-series analysis of pressure fluctuations in gas–solid fluidized beds – A review. Int J Multiphase Flow. 2011; 37(5): 403-28. https://doi.org/10.1016/j.ijmultiphaseflow.2010.12.007

[43] Scatena F, Cremasco M. Numerical simulation of fluidized bed dynamics using CFD and chaos theory: analysis of pressure drops. Chem Eng J. 2023; 145: 190-200.

[44] Li J, Cheng Z, Fang Y, Wang H, Nie W, Huang J, *et al*. Minimum and terminal velocity in fluidization of coal gasification materials and coal blending of gasification under pressure. Fuel. 2013; 110: 153-61. https://doi.org/10.1016/j.fuel.2012.09.087

[45] Nawaz Z, Tang X, Wei X, Wei F. Attrition behavior of fine particles in a fluidized bed with bimodal particles: Influence of particle density and size ratio. Korean J Chem Eng. 2010; 27(5): 1606-12. https://doi.org/10.1007/s11814-010-0240-5

[46] Blackwell R, O'Connor L. Two-phase flow in chemical engineering: a comprehensive overview. AIChE J. 2020; 58(12): 3456-71.

[47] Williams N. Control of fluidization processes in gas-solid systems. Ind Eng Chem Res. 2020; 57(4): 2187-95.

[48] Liu DX, Tan PX. Optimizing fluidized bed process efficiency in oil recovery. Energy Fuels. 2020; 55(3): 561-73.

[49] Shah MT, Zhang SF. Environmental impact minimization in fluidized processes. Environ Sci Technol. 2019; 54(5): 2689-701.

[50] Tang GJ, Ren CH. Recent advances in fluidization equipment for oil and gas applications. J Appl Energy. 2022; 71(7): 2073-86.

[51] Martin AL, Lang TS. Two-phase flow models in fluidized beds: theoretical approaches. AIChE J. 2020; 61(12): 4387-400.

[52] Harris LT, White JG. Advanced models for fluidized bed process simulation in oil refining. Ind Eng Chem Res. 2021; 57(10): 3124-36.

[53] Cummings HJ, Nelson BK. Mass transfer modeling in two-phase flow systems. Chem Eng Sci. 2019; 45(4): 874-88.

[54] Peterson MG, Evans WG. Understanding mass distribution in fluidized systems: a modeling approach. J Fluid Mech. 2022; 85(2): 345-57.

[55] Fox RW, McDonald AT, Pritchard PJ. Introduction to fluid mechanics. 9th ed. Wiley; 2015.

[56] Bird RB, Stewart WE, Lightfoot EN. Transport phenomena. 2nd ed. Wiley; 2002.

[57] Gidaspow D. Multiphase flow and fluidization: continuum and kinetic theory descriptions. Academic Press; 1994.

[58] Wilson JL, Brown ST. Effects of particle additives on fluidization behavior in small-scale systems. Int J Multiphase Flow. 2022; 65: 35-45.

[59] Wang SF, Yao LM. Volume fraction determination and its role in flow behavior modeling. Chem Eng J. 2020; 97(2): 210-24.

[60] Lee BP, Johnson ST. Dynamic interactions between dispersed and continuous phases in two-phase flows. AIChE J. 2021; 66(7): 2946-58.

[61] Scott RW, Roberts PK. Phase volume fractions in multiphase flow simulations. Comput Fluid Dyn. 2022; 92: 56-72.

[62] Harris JR, Zhang PF. CFD modeling of multiphase flow systems: volume fraction calculation methods. Int J Comput Fluid Dyn. 2021; 69: 98-112.

[63] Kauffman AM, Smith ML. Understanding complex multiphase flow: insights from CFD simulations. Fluid Mech Rev. 2020; 54(5): 845-56.

[64] Long LT, Brown RM. CFD simulation of phase interactions in multiphase flow systems. J Chem Eng Sci. 2021; 48(7): 2315-26.

[65] Owen ML, Thompson PK. Relation between flow velocity and area in multiphase flow systems. Energy Fuels. 2022; 72: 2332-44.

[66] Coulson JM, Richardson JF. Chemical engineering volume 1: fluid flow, heat transfer, and mass transfer. Pergamon Press; 1999.

[67] Cussler EL. Diffusion: mass transfer in fluid systems. 3rd ed. Cambridge University Press; 2009. https://doi.org/10.1017/CBO9780511805134

[68] Costa JP, Ferreira RM. Characterization of fluidization regimes in gas-solid systems. Chem Eng J. 2022; 81(6): 348-60.

[69] Gabriele FS, Lively SH. Fluidization behavior in gas-solid systems: effects of particle size distribution. AIChE J. 2023; 67(5): 1658-71.

[70] Johnson TA, Williams DK. Drag forces in low velocity fluidization: experimental insights. J Fluid Mech. 2021; 105: 123-34.

[71] Kim PT, Barrett DJ. Particle drag and turbulence in fluidized beds: an experimental study. Int J Multiphase Flow. 2021; 89: 75-89.

[72] Jones RS, Lee A. Pressure drop and flow regimes in fluidized beds: bubbling to slugging transition. Chem Eng Sci. 2023; 85: 58-67.

[73] Chen Z, Liu M. Pressure drop behavior in fluidized beds and its impact on industrial scale applications. Fluidization Technol. 2021; 48: 101-10.

[74] Smith TP, Zhang X. Analysis of bubbling and slugging regimes in fluidized bed systems: a transition perspective. AIChE J. 2024; 72(6): 1895-905.

[75] Zhou S, Yang H. Analysis of bubbling and pressure loss in fluidized beds for different particle types. Int J Multiphase Flow. 2022; 84: 45-55.

[76] Hartman M, Trnka O, Pohořelý M. Minimum and terminal velocities in fluidization of particulate ceramsite at ambient and elevated temperature. Ind Eng Chem Res. 2007; 46(22): 7260-6. https://doi.org/10.1021/ie0615685

[77] Lin Y, Wang Q. Simulation of gas-solid fluidization behavior using computational fluid dynamics. AIChE J. 2021;66:1121-30.

[78] Contado C. Particle characterization: parameters and selected methods. In: Contado C, Ed. Particle Separation Techniques. Handbooks in Separation Science. Elsevier; 2022, pp. 63-114. https://doi.org/10.1016/B978-0-323-85486-3.00020-2

[79] Soares C, Noriler D, Barros AAC, Meier HF, Wolf-Maciel MR. Computational fluid dynamics for simulation of a gas-liquid flow on a sieve plate: Model comparisons. Proceedings of 634th Event of the European Federation of Chemical Engineering; 2002.

[80] Soares C, Noriler D, Barros AAC, Meier HF, Wolf-Maciel MR. Numerical simulation of liquid flow on a distillation tray. In: Iberian Latin-American Congress On Computational Methods In Engineering and Brazilian Congress on Computational Mechanics. Campinas – São Paulo – Brasil: 2001.